Equilibration of crystal surfaces

W. Selke
Institut für Festkörperforschung-Forschungszentrum Jülich, D-52425 Jülich, Germany

P. M. Duxbury
Department of Physics and Astronomy and Center for Fundamental Materials Research, Michigan State University, East Lansing, Michigan 48824-1116

(Received 29 June 1995)

The relaxation towards equilibrium of various profiles imprinted on a crystal surface is studied above and below the roughening temperature of that surface. Evaporation kinetics and, above roughening, surface diffusion are considered. Continuum theory and step models are compared with the results of Monte Carlo simulations. Above roughening, the simulational data are well understood in the framework of the continuum theory, and the oscillatory profiles characteristic of surface diffusion are easily seen. Below roughening, the current continuum theories do not treat the top-step annihilation process correctly. That process is described using a Langevin theory for step fluctuations. In addition, the opposing effects of the anisotropic mobility and surface free energy on the profile shapes are emphasized and illustrated in a phenomenological extension of the continuum theory with small rounding parameters. Although these extensions of the continuum theory improve understanding of the Monte Carlo data below roughening, finite-size and lattice effects still preclude a quantitative fit of the theory to the Monte Carlo data.

I. INTRODUCTION

A profile imprinted on an initially flat equilibrium crystal surface will undergo morphological changes when relaxing towards equilibrium. This morphological evolution has been found, both experimentally and theoretically, to be significantly different above and below the roughening transition of the relevant crystal surfaces.[1–6]

These healing processes have been studied most extensively for one-dimensional gratings [see Fig. 1(a)]. Above roughening, the gratings acquire, for small amplitude to wavelength ratios, a sinusoidal form, as predicted by the classical capillary theory of Mullins[1] and confirmed by experiments[3] and simulations.[5–10] The decay of the amplitude is, asymptotically, exponential in time. This is true for both evaporation dynamics and (experimentally more relevant) for surface diffusion.

Below roughening, extensions of the classical continuum theory[2,11–16] take into account the anisotropic surface free energy, $\sigma(\theta)$, and mobility, $m(\theta)$, which may be singular at special orientations of the surface. These anisotropies may play opposing roles.[6] An increase of the surface tension with the inclination angle (away from a special orientation at $\theta=0$), may lead to a broadening of the profile shape at its maxima and minima, or even a faceting in the case of a cusplike singularity. On the other hand, the profile may sharpen at the sides and near the apexes due to a lowering of the mobility (or diffusion coefficient) at decreasing angles. Therefore, the resulting morphological evolution will depend crucially on the balance of these two competing tendencies of broadening and sharpening.

In fact, different scenarios have been suggested, based on extensions of Mullins' theory. For surface diffusion, Bonzel and co-workers[15] obtained numerically a pronounced broadening of the profile surface, when regularizing the cusp singularity of the free energy, assuming an isotropic mobility (or diffusion coefficient). That assumption has also been made by Spohn,[2] who kept the singularity in $\sigma(\theta)$, giving rise to a faceting at the top and bottom of the profile, and a finite decay time. In marked contrast, in the continuum description of Rettori and Villain,[12,13] the sharpening tendency prevails, with profiles being sharper than parabola near the top. For evaporation dynamics, both Spohn[2] as well as Lançon and Villain[11] predict a similar sharpening, caused by a linear vanishing of the mobility, $m \sim |\theta|$, on approach to the flat surface orientation. However, the nonparabolic profiles following from these continuum theories are not seen in Monte Carlo simulations.[5–10] In addition, the simulated profiles and their decay typically reflect the atomistic nature of the shape evolution, not captured by the continuum descriptions, as seen in the dynamics of the top terraces of the gratings and their bounding steps, with meandering of the steps as well as forming and shrinking of islands.[5,6] Experimentally, below roughening, broadening or even faceting has been reported, for instance, for gold[3] and silicon[4] surfaces, where the healing proceeds, predominantly, through surface diffusion.

In this contribution, we shall study the relaxation of several initial profiles imprinted on a crystal surface, considering surface diffusion above roughening and evaporation dynamics both above and below roughening. Previous Monte Carlo work has been on gratings, so here we concentrate on wire and bump profiles [Figs. 1(b) and 1(d)], for which continuum theory predictions exist and which have not been tested by simulations. The pertinent

continuum theories are outlined in Sec. II. Section III contains a discussion of two new aspects that are relevant in comparing continuum theory with simulations or experiment. The first is the dynamics of step annihilation at the top of profiles such as the wire or grating. The second is the role of finite-size effects or small rounding parameters on the opposing effects of the mobility and surface free energy. In Sec. IV the Monte Carlo data are presented and discussed. A summary concludes the article.

II. CONTINUUM THEORY

We consider the relaxation of the profiles of Fig. 1, where $z(x,y)$ is the height of the surface at the point x,y.

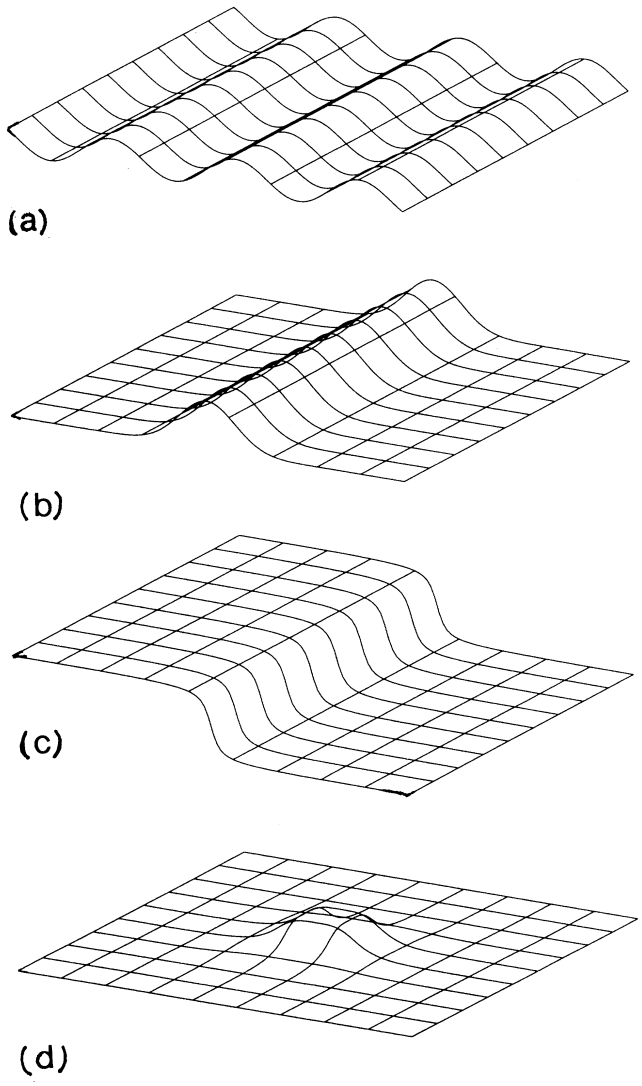

FIG. 1. Sketch of the initial profiles. (a) 1D grating; (b) 1D wire; (c) 1D step; (3) 2D bump.

A. Evaporation recondensation above roughening

The continuum theory for surface relaxation is well established, and is based on the seminal work of Herring and Mullins.[1] In this theory, the surface evolution is driven by local deviations from the equilibrium chemical potential. In the case of evaporation recondensation, the governing equation is

$$\mathbf{v}_n = -m\mu\hat{n} \ , \tag{1}$$

where $\mathbf{v}_n$ is the normal velocity at a point on the surface, m is the mobility, and μ is the local deviation of the surface chemical potential from the equilibrium value. The "gas" or reservoir with which particle exchange is occurring is assumed to be at the equilibrium chemical potential everywhere. The deviation μ is almost always assumed to be small, so it can be found from a variation of the equilibrium free energy. Using this principal, one obtains

$$\mu=\Omega\left[\left[\sigma+\frac{\partial^2\sigma}{\partial\theta^2}\right]\kappa_1+\left[\sigma+\frac{\partial^2\sigma}{\partial\phi^2}\right]\kappa_2\right] , \tag{2}$$

where $\sigma(\theta,\phi)$ is the free energy of a surface oriented at angles θ, ϕ to a reference [e.g., (111) of a fcc metal] surface, κ_1 and κ_2 are the principle curvatures of the surface, and Ω is a volume element. The mobility m is not so well understood, although in some limiting cases (see below) its behavior has been argued to be quite simple.[2,10] In the thermodynamic limit, the surface free energy below the roughening temperature (T_R) exhibits cusps at special orientations, so care has to be taken in analyzing Eq. (1) in that limit [because at cusp orientations the second derivative in (2) yields singularities]. Although it may be well known, we first summarize the behavior in the small-slope approximation where Eqs. (1) and (2) reduce to a linear diffusion equation, for convenience of later comparison to the Monte Carlo data.

In this limit, valid at sufficiently high temperatures and low amplitudes, $z_x=\partial z/\partial x$ and $z_y=\partial z/\partial y$ are assumed to be small, and the surface free energy and the mobility are taken to be isotropic, i.e., we replace them by constants (σ_0 and m_0). Using these approximations in (1) and (2) leads to the linear diffusion equation

$$\frac{\partial z}{\partial t}=E\nabla^2 z \ , \tag{3}$$

where

$$E=p_0\sigma_0\Omega/[(2\pi M)^{1/2}(k_B T)^{3/2}] \ , \tag{4}$$

with p_0 being the equilibrium gas pressure, $k_B T$ the Boltzmann constant times the temperature, σ_0 the free energy of the reference surface, and M the mass of a particle. The asymptotic "scaling" solutions to this equation for the four cases of Fig. 1 are as follows. For the one-dimensional (1D) grating [Fig. 1(a)],

$$z(x,t)\sim e^{-(2\pi/\lambda)^2 Et}\sin(2\pi x/\lambda) \ , \tag{5}$$

where λ is the wavelength of the grating, and the grating

amplitude decays as $e^{-(2\pi/\lambda)^2 Et}$. The solution for the 1D wire [Fig. 1(b)] is

$$z(x,t)\sim\frac{e^{-x^2/4Et}}{\sqrt{t}}\ , \tag{6}$$

so that the wire amplitude decays as $1/t^{1/2}$ and its width increases as $t^{1/2}$. The 1D step [Fig. 1(c)] behaves as

$$z(x,t)\sim\int_{-\infty}^{x}\frac{e^{-p^2/4Et}}{\sqrt{t}}dp\ , \tag{7}$$

so that its width increases as $t^{1/2}$. Finally, the 2D bump [Fig. 1(d)] decays according to

$$z(r,t)\sim\frac{e^{-r^2/4Et}}{t}\ , \tag{8}$$

so that this profile spreads as $t^{1/2}$ and decays as $1/t$.

B. Surface diffusion above roughening

Again following Herring and Mullins,[1] it is known that surface diffusion is driven by gradients in the local surface chemical potential,

$$\mathbf{v}_s=-m_{sd}\nabla_s\mu\ , \tag{9}$$

where m_{sd} is the surface mobility, and ∇_s is the surface gradient. In combination with the continuity equation,

$$\mathbf{v}_n=-\Omega\nabla_s j_s\ , \tag{10}$$

where $j_s=nv_s$ (with n the adatom density), one obtains

$$\mathbf{v}_n=\Omega\nabla_s n m_{sd}\nabla_s\mu\ . \tag{11}$$

Assuming the small-slope limit, leads to the linear fourth-order equation,

$$\frac{\partial z}{\partial t}=-F\nabla^4 z\ , \tag{12}$$

where $F=D_s\sigma_0\Omega^2 n/k_BT$, with D_s being the surface diffusion constant. This equation has been used extensively to describe the dynamics of surfaces, for example, grain boundary grooving, sintering, and profile evolution. The results, found using Fourier analysis, are not as straightforward as for the evaporation-recondensation case. In any event, the asymptotic temporal decay laws are known analytically, and for the four profiles of Fig. 1 they are the following:[17] for the 1D grating, amplitude $\sim e^{-(2\pi/\lambda)^4 Ft}$; for the 1D wire, amplitude $\sim t^{-1/4}$ and width $\sim t^{1/4}$; for the 1D step, width $\sim t^{1/4}$; and for the 2D bump, amplitude $\sim t^{-1/2}$ and width $\sim t^{1/4}$.

It is seen that the characteristic exponent for profile decay by surface diffusion above roughening is one-half of that for evaporation-recondensation dynamics. Another interesting feature of profile decay by surface diffusion is that some of the profiles develop oscillations as they decay. This feature will be illustrated in the Monte Carlo simulations of Sec. IV.

It is well known that as one approaches T_R from above, a cusp in the surface free energy develops. Therefore, slightly above T_R a strongly anisotropic surface free energy may be expected. Indeed, in the exactly solvable one-dimensional (solid-on-solid) SOS model it is easy to show[9] that the "cusp" is round only for angles smaller than $\theta_0\sim e^{-J/k_BT}$. The validity of the linear theories, Eqs. (3) and (12), is then restricted to small amplitudes such that $\theta<\theta_0$ everywhere on the profile. At larger angles, the profile shape and dynamics are affected by anisotropy, as had been demonstrated by simulating 1D gratings at various temperatures and amplitudes.[9]

C. Evaporation recondensation below roughening

In this limit, the continuum surface free energy is singular and near a cusp orientation has the form

$$\sigma(\theta)\sim G_1|\theta|+G_3|\theta|^\gamma \tag{13}$$

at low angles $|\theta|$. The first term in Eq. (13) is due to the free-energy cost of creating an atomic step, while the second term is due to step-step interactions. Both elastic interactions and entropic interactions lead to $\gamma=3$. In addition, below roughening, the mobility m in Eq. (1) is dominated by the rate at which atoms detach from step edges. This simple argument suggests that

$$m\sim\nu e^{-\Delta/k_BT}|\theta|=e_1|\theta|\ , \tag{14}$$

where Δ is an activation energy for atoms from, e.g., kink sites, and ν is an attempt frequency (e.g., the Debye frequency). It has been assumed[2] that (14) captures the essence of the mobility behavior at low temperatures and on approach to a cusp orientation (note that Hager and Spohn also considered, in the more recent work,[2] the consequences of different forms of the mobility, motivated by the conflicting simulational findings). For one-dimensional profiles [Figs. 1(a)–1(c)], combining Eqs. (1) and (2) with (13) and (14), one obtains[2,11]

$$\frac{\partial z}{\partial t}=a_1 z_x^2 z_{xx}\ , \tag{15}$$

where $a_1=e_1(G_1+6G_3)\Omega$. Similarly for two-dimensional cases with cylindrical symmetry, the governing equation is[2]

$$\frac{\partial z}{\partial t}=a_1 z_r^2 z_{rr}+\frac{9G_3e_1z_r^3}{r}+\frac{G_1e_1z_r}{r}\ . \tag{16}$$

The asymptotic behavior of (15) and (16) can be found using separation or variables or similarity solutions.[2] The result for the 1D grating is

$$z(x,t)\sim(t/\lambda^2)^{-1/2}\Psi_1(x/\lambda)\ , \tag{17}$$

so that its amplitude decays as $(t/\lambda^2)^{-1/2}$. The 1D wire behaves as

$$z(x,t)\sim t^{-1/6}\Psi_2(xt^{-1/6})\ , \tag{18}$$

so that its amplitude decays as $t^{-1/6}$ and its width $\sim t^{1/6}$. Note that the profiles of the wires and the gratings display a nonparabolic sharpening at their apexes, with $\delta z\sim(\delta x)^{4/3}$. That sharpening has not been observed in previous Monte Carlo simulations of grating decay, nor is it seen in the simulations of wires presented in Sec. IV. Reasons for this discrepancy will be discussed in Sec. III.

Essentially, the top-step annihilation process is not taken into account in Eq. (14). This problem does not occur for the 1D step, and Eq. (15) is expected to provide a reasonable description. The profile is then given by

$$z(x,t)\sim\Psi_2(xt^{-1/4}) , \tag{19}$$

and so its width spreads $\sim t^{1/4}$. Finally, the 2D bump is predicted to follow, in the limit of small amplitudes, the scaling form

$$z(r,t)\sim\Psi_4[\sqrt{(ct+r^2)}] . \tag{20}$$

Here the first term of the right-hand side of Eq. (16) is dominant, describing the independent decay of the curved steps. At large amplitudes, the step-step interactions, contained in the remaining two terms of that equation, will alter the behavior. The Monte Carlo data (see Sec. IV) are consistent with this prediction.

In contrast to the behavior above roughening, different initial profiles may relax in qualitatively distinct ways. For example, an initial 2D bump [Eq. (20)] will eventually *shrink* as its amplitude decays; on the other hand, at $T>T_R$, one observes the usual spreading. The shrinking is due to the presence of steps with a net curvature below roughening, and this leads to enhanced step-edge evaporation.

III. CUSP-ROUNDING MECHANISMS AND PROFILE DECAY BELOW ROUGHENING

Below roughening, the 1D step and the 2D bump may be described quite well by the continuum theory which follows from Eqs. (15) and (16), respectively. However, for 1D gratings and 1D wires, that theory implies the supposedly unphysical feature of a sharp apex in the profile shape. In this section we mention and discuss mechanisms which may round this sharp apex in simulations and in experiment. Such mechanisms are, in particular, the following.

(i) *Miscut.* If the surface is miscut, the closest approach to the cusp orientation that is achieved is the miscut angle α. The ideal behavior, Eqs. (17) and (18), is then rounded out at an angle $\theta_0=\alpha$. The drastic effect of this on-profile decay has been illustrated before[11] for 1D gratings, with the nonparabolic sharpening near the top being replaced by a pronounced broadening. Of course, the discrepancy between continuum theory and the simulations cannot be explained by a miscut, because the Monte Carlo studies were done on perfect surfaces.

(ii) *Finite-size effects and top-step dynamics.* One would always anticipate finite-size effects, present and possibly much pronounced in simulations, which would round the ideal cusps of Eqs. (13) and (14). In addition, it is easily seen that the mobility $m\geq 1/l_{\rm top}$, where $l_{\rm top}$ is the width of the top terrace, because the two steps that bound the top terrace act as sources of adatoms.[9] In the case of 1D gratings, the smallest possible mobility is always greater than $1/\lambda$, in contrast to the vanishing mobility at the top assumed by the continuum theory, Eq. (15). Indeed, implicit in the continuum theory for the 1D grating and the 1D wire is the assumption that the center of masses of the two unlike steps at the profile apexes undergo contact annihilation. However, that is not the case. Instead, the step annihilation begins when the two fluctuating steps first make contact,[5,9] which implies a longer-range annihilation process. We shall illustrate this aspect in the following.

A. The effect of rounding the free energy and mobility

We first assess, in a phenomenological way, the effect of rounding both the mobility singularity and the surface free-energy singularity, due to, e.g., possible finite-size effects. To do this we introduce two rounding angles, θ_m and θ_f, into the expressions (13) and (14), so that

$$m\sim e_1(\theta^2+\theta_m^2)^{1/2} , \tag{21}$$

and similarly we make the replacement

$$|\theta|\rightarrow(\theta^2+\theta_f^2)^{1/2} . \tag{22}$$

In general $\theta_m\neq\theta_f$, and the limiting behavior Eq. (15) may be recovered when both of these rounding parameters approach zero. From Eqs. (1) and (2) it follows, for 1D profiles,

$$\frac{\partial z}{\partial t}=a_1(\theta^2+\theta_m^2)^{1/2}\frac{z_{xx}}{(1+z_x^2)}\left[G_0+\frac{G_1[(\theta^2+\theta_f^2)^2+\theta_f^2]}{(\theta^2+\theta_f^2)^{3/2}}+\frac{G_3[(\theta^2+4\theta_f^2)^2+6\theta^2+3\theta_f^2]}{(\theta^2+\theta_f^2)^{1/2}}\right] . \tag{23}$$

A constant G_0 has been added to the surface free energy, as occurs in lattice models and experiment. Note that the equation is formally similar to the continuum theory above, but close to roughening; there the rounding is due to thermal fluctuations. It is readily seen that if the slope (amplitude) of the profile is small, $z_x\ll\min(\theta_m,\theta_f)$, then the equation becomes linear, and the profile decay is like that given by Eq. (3). In that limit, the effective diffusion constant depends on the small rounding parameters, being proportional to $a_1\theta_m(G_0+G_1/\theta_f)$. For larger slopes (amplitudes), the 1D grating and wire profiles may broaden at their tops to take advantage of the lower free energy there. This cannot occur in the continuum description of Eq. (15), because there a possible broadening or even faceting is (over)compensated by the sharpening tendency caused by the vanishing mobility at the apexes. Certainly, in our description the anisotropy of the mobility still favors a more rapid decay of parts of the

profile with larger angles. This may produce leaner forms at the sides of the profile and also a sharpening near the top, but with parabolic shapes. Accordingly, the actual profile shape reflects the interplay of these two opposing effects stemming from the surface free energy and the mobility. Their relative impact is determined, in the phenomenological description, by the concrete choice of the small rounding parameters. An example is depicted in Fig. 2, with θ_m larger than θ_f. Starting with a sinusoidal grating, the sharpening tendency dominates at early times. Eventually one observes a broadening near the top, before the profiles acquire again, asymptotically, the sinusoidal form of the linear solution at sufficiently small amplitudes. Figure 2(b) shows the amplitude decay as a function of time, and from this figure, it is seen that at long times (low amplitudes), the exponential decay law of the linear theory is recovered.

Note that a similar phenomenological ansatz, taking into account, however, only a small rounding parameter for the surface free energy, assuming an isotropic nonzero mobility, has been analyzed before,[15] for surface diffusion. In that way, experimentally determined profiles could be reproduced successfully.

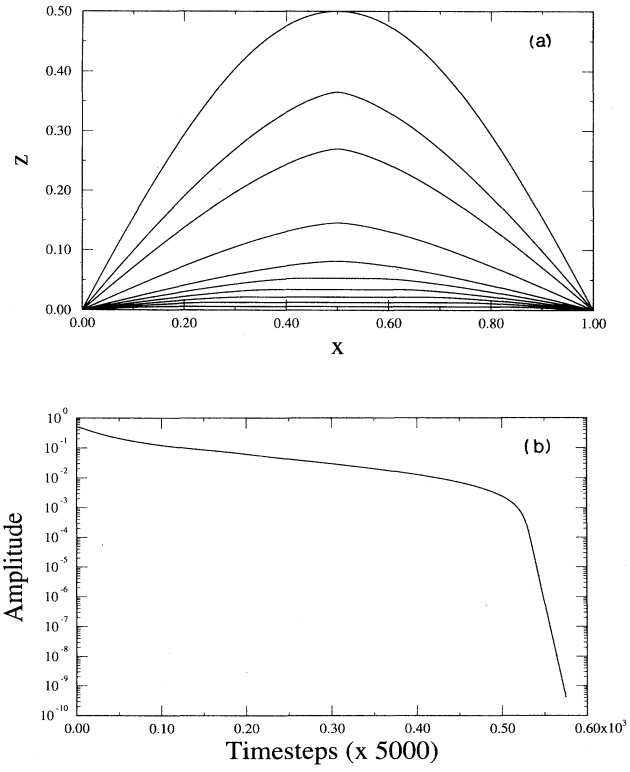

FIG. 2. The effect of small parameters on the decay of a 1D grating. (a) Profile shape as a function of amplitude. (b) Profile amplitude as a function of time. Solutions are for $\theta_m = 0.005$, $\theta_f = 0.001$, $G_0 = G_1 = G_3 = 1.0$, using an explicit time integration of Eq. (23) with 160 points and central differences in the x direction. The amplitude is in lattice units, while the time is in dimensionless units.

B. The top-step annihilation process

Two wandering steps, bounding the top terrace of a 1D grating or wire, may annihilate each other by first touching, then forming islands, and finally by island shrinking.[5,9] This process drives the equilibration process. Its main characteristics may be mimicked by a single step being repelled from a hard wall and being absorbed by an attractive wall. Thus, consider a system of these two straight walls, at distance W, and of length L, with a step which is initially flat and located near the repelling wall. The steps begin to wander with the step fluctuations growing proportional to $t^{1/4}$ and moving the step away from the hard wall.[18,19] Once a fluctuation of the step first touches the attractive, absorbing wall, it attaches and that produces a net local curvature near the point of contact. The curvature is of order $1/W$. This curvature causes a more rapid attachment of the remaining nonabsorbed parts of the step according to the law,

$$\frac{dl_s}{dt} = -\frac{m_2 \sigma_s \Omega}{W} \quad \text{for } l_s \gg W \ , \tag{24}$$

where l_s is the length of the step which is still not absorbed by the wall, m_2 (assumed constant) is the step mobility, and σ_s (assumed constant) is the step free energy. This leads to a linear decay, in time, of l_s. It follows that the time taken for the curvature-driven annihilation of the step *from single initiation points* (corresponding to the time for island shrinking in the original problem) is approximately LW, while the time taken for the step to first touch the absorbing wall (the time needed for the meandering top steps to meet) is approximately W^4. Thus there are two distinct regimes. If $L \ll W^3$, the dominant time is the time for first attachment, with the top terrace annihilating rapidly once that attachment is made. However if $L \gg W^3$, many attachments occur and many islands shrink over a time scale of order W^4. In both cases the time taken for the top step to annihilate is of order W^4. We have simulated this process using the usual stochastic Langevin equation $\Gamma^{-1}\partial h/\partial t = \sigma \nabla^2 h + \eta(t)$, with the step bounded between a hard wall and an absorbing wall. The absorbing wall is distance W from the hard wall, and at $t=0$, the step is flat and located close to the hard wall. The results are presented in Fig. 3, where we have set the rate $\Gamma = 1$, the step free energy $\sigma = 1$, and the noise amplitude is also 1. In particular, it is seen that the island shrinking time (crosses) dominates for small W, while the attachment time (pluses) dominates for large W. In the regime $1 \ll W^2 \ll L$, $\tau \sim W^4$ is found, while the crossover to a smaller exponent occurs at larger W due to finite-size effects (in the limit $L \ll W^2$, the step can be treated as a single walker at the center of mass of the string, in which case $\tau \sim LW^2$).

From the discussion above, it is seen that in the vicinal limit ($L \to \infty$; $W \to \infty$, with $W^2 \ll L$), two steps annihilate in a time of order W^4, where W is the step separation. The topology of the top terrace consists of many islands if $L \gg W^3$, while only one or a few islands occur if $L \ll W^3$.

Note that the dynamics of single steps has received much attention recently, motivated largely by scanning tunneling microscopy[20–22] (STM).

IV. MONTE CARLO SIMULATIONS

The standard microscopic model for a surface displaying a roughening transition is the SOS model, with the Hamiltonian

$$H=\sum_{l,m} J|h_l-h_m| \tag{25}$$

where h_l denotes the height, taking integers only, at site l of the surface above a flat reference plane. The interaction between neighboring sites, l and m, is determined by the bonding energy J. Below the roughening transition temperature, $T<T_R$, the surface is smooth; in the rough phase, $T>T_R$, the height fluctuations diverge, in the limit of an infinitely extended surface.

For a square lattice, i.e., the surface of a cubic crystal, T_R is known to be $k_B T_R/J\approx 1.24$,[23] where k_B is the Boltzmann constant. To study properties above roughening, it is also convenient to consider the one-dimensional SOS model, where $T_R=0$.

The relaxation of an initial profile, imprinted on the surface, towards thermal equilibrium, $\langle h_l\rangle=0$, may be simulated by Monte Carlo algorithms corresponding to particle transport by evaporation condensation and by surface diffusion.[5–10] In the case of evaporation dynamics, Glauber kinetics is employed. Surface diffusion is described by Kawasaki kinetics, i.e., hopping of surface atoms to neighboring sites. The trial site is chosen randomly for both Glauber and Kawasaki kinetics.

Above roughening, both types of dynamics were simulated. Below roughening, only results for evaporation kinetics will be presented; surface diffusion becomes extremely slow, and it seems difficult to obtain data of the desired accuracy.[5,8,24]

We considered the relaxation of 1D wires and 2D bumps.

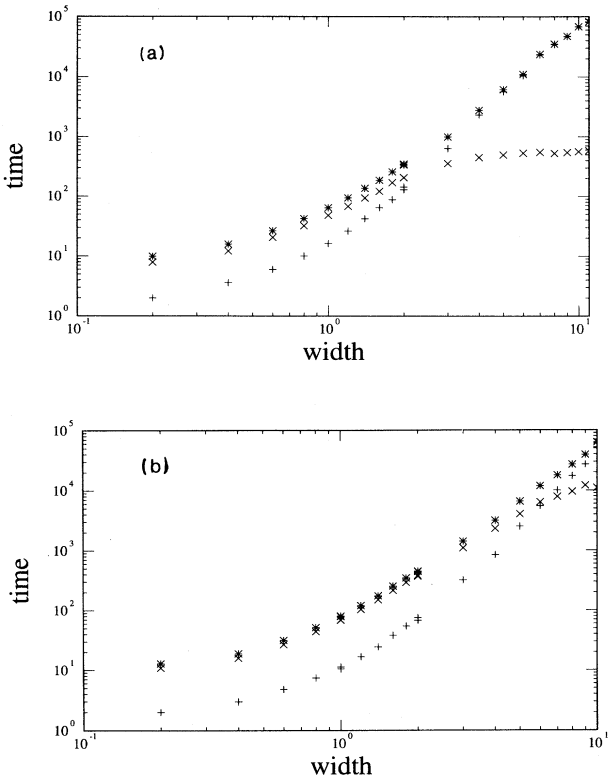

FIG. 3. The time, in dimensionless units, taken for a step to be absorbed by an absorbing wall. Asterisks are the total time to absorb (total time), pluses indicate the time taken for the first attachment of the step (first attachment time), and the crosses are the time taken for the islands to shrink once they have begun forming (islanding time). The islanding time plus the first attachment time is equal to the total time. W (in dimensionless units) is the initial distance between the step and the absorbing wall, and the time step is 0.5. (a) $L=100$ (averaged over 50 configurations) and (b) $L=1000$ (10 configurations).

A. 1D wire profiles

We first discuss the Monte Carlo findings for 1D wires. Simulation results for one- and two-dimensional SOS models were obtained. In one dimension, with $(2K+1)$ equidistant sites at $x=-K,-K+1,\ldots,K-1,K$, the initial configuration may be defined as

$$h(x,t=0)=\begin{cases}0, & |x|>M\\ A_0, & |x|\le M\end{cases} \tag{26}$$

describing a wire of height A_0 and width $w_0=2M+1$. For a rectangular surface of $(2K+1)\times L$ sites, (x,y), the analogous geometry is chosen, with the wire being extended in the y direction, $h(x,y,t=0)=h(x,t=0)$. In both dimensions, full periodic boundary conditions are used.

To characterize the morphological changes, we recorded the profile $z(x,t)$ by averaging $h(x,y,t)$ over many realizations of the healing process at time t (see Ref. 5); typically we sampled over 10^4 to 10^6 realizations. The time scale is set by the number of Monte Carlo steps per site (MCS/S). Various features of the profile may be of interest, for instance, the amplitude $A(t)=z(x=0,t)$ and the width.

Above roughening, surface diffusion was simulated for the one-dimensional case, while evaporation kinetics was studied for one- and two-dimensional surfaces. The initial height A_0 of the 1D wire was, in most cases, chosen to be 3 or 5, with the initial width w_0 ranging from 3 to 11. The size of the surface varied from $(2K+1)=41$ to 101, with L being, usually, equal to 41. Relaxation was recorded, in the one-dimensional case, at $k_BT/J=0.8$ and, in the two-dimensional case, at $k_BT/J=1.5$ and 2.0.

We present first our findings for evaporation dynamics. Examples of profile shapes are depicted in Fig. 4, showing Monte Carlo data for the one-dimensional surface together with numerical solutions of Eq. (3), using the same initial shape. From that figure, one observes a, perhaps

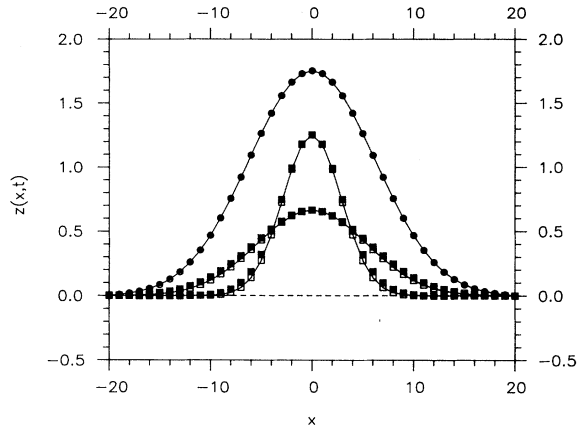

FIG. 4. Simulated wire profiles of the one-dimensional SOS model at $k_BT/J=0.8$ (full symbols), compared to those of Mullins' theory (open symbols), for evaporation kinetics. Initial wire configurations with $A_0=w_0=3$ (squares) and with $A_0=3$ and $w_0=9$ (circles) are considered. The solid line connects the points of the continuum theory. The amplitude and x coordinate are in lattice units, while the profiles were calculated after 76 MCS/site (top curve), 21 MCS/site (second curve), and 78 MCS/site (smallest amplitude curve), averaging over 10^6 realizations.

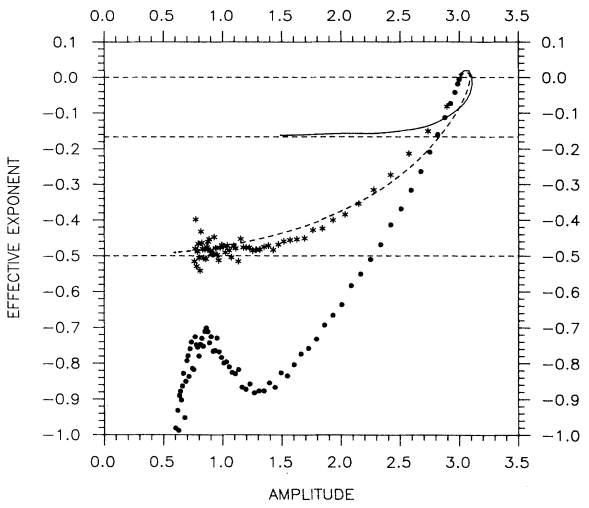

FIG. 5. Effective exponent, Eq. (28), versus height of the wire profile, from simulations of the two-dimensional SOS model, with $A_0=w_0=3$, above (asterisks), $k_BT/J=2.0$, and below (full dots), $k_BT/J=0.8$, the roughening transition, compared to results from the corresponding continuum theories above (broken line) and below (solid line) the transition, for evaporation kinetics.

surprisingly, close agreement between the simulated shapes and the forms predicted by Mullins' asymptotic continuum theory. Presumably, much of the remaining difference could be described by including the actual slopes of the profile shape and the anisotropies of σ and m in the continuum description [see Eqs. (2) and (23)],

$$\frac{\partial z}{\partial t}=\tilde{E}m(\theta)[\sigma(\theta)+\sigma''(\theta)]\frac{z_{xx}}{1+z_x^2}\ . \tag{27}$$

The anisotropies of the mobility and the surface free energy are expected to become less important at higher temperatures and for smoother profiles, as had been confirmed before for 1D gratings (periodic grooves).[9] Indeed, we found that the agreement improved for wider profiles and at smaller amplitudes, as may be inferred from Fig. 4. As described above, the anisotropies of σ and m play opposing roles, and a compensation effect may further contribute to the striking similarity of the simulated and the predicted limiting profiles. Hardly visible systematic deviations (the simulated profiles are always slightly broader than the predicted ones, at small amplitudes) can be attributed to the small differences in the amount of mass change during the healing process; see below.

The asymptotic validity of Mullins' theory, Eq. (3), may also be seen from the time dependence of the relaxation process. To describe the decay of the amplitude $A(t)$, one may define an effective exponent τ by

$$\tau=\ln[A(t)/A(t+\Delta t)]/\ln[t/(t+\Delta t)]\ , \tag{28}$$

where Δt is a time increment measured in MCS/S. From Fig. 5, we see that $\tau=\tau(A)$ approaches the asymptotic value $\tau_0=-\frac{1}{2}$, at small amplitudes, both for the simulated data and in continuum theory. Note that in continuum theory the initial rectangular profile gets curved very quickly, associated with a significant increase in the amplitude. In the simulations, there is no mechanism for that amplitude increase.

Similar observations hold for two-dimensional surfaces above roughening. The simulated shapes of wires with small or moderate initial amplitude and width, at temperatures well above the transition, follow closely the asymptotic forms predicted by Mullins' theory. Again the small differences between continuum theory and simulations can be attributed to anisotropies in the mobility and surface free energy. However, for both, the exact expressions are not known.

In the case of surface diffusion, the agreement between simulational data and the capillary theory reaffirms the above conclusion that the classical theory, Eq. (12), provides a good description even for surface perturbations of the extent of a few lattice spacings at temperatures well above the roughening transition and for small amplitude (slope) profiles; see Fig. 6. Correction terms are either small or tend to compensate each other. In particular, the oscillatory shape[1,17] of the profile, which follows from Eq. (12), is nicely reproduced in the Monte Carlo simulations. The height is found to decay more slowly than for evaporation dynamics, $A(t)\propto t^{-1/4}$ at late times, in agreement with the continuum theory (see Sec. II). The width of the profile, measured by the distance between the minima to the left and right of the central maximum, increases in proportion to $t^{1/4}$, again in accordance with continuum theory. Of course, by extending the continuum theory to include arbitrary slopes of the profile and

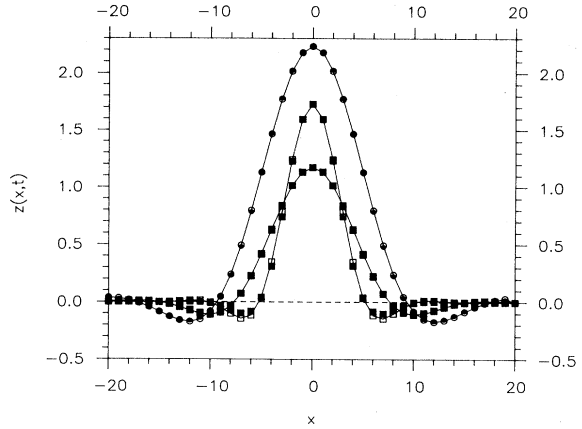

FIG. 6. Wire profiles of the one-dimensional SOS model, with $A_0=w_0=3$ (full squares), and with $A_0=3$ and $w_0=7$ (full circles), at $k_BT/J=0.8$, simulating surface diffusion, compared to Mullins' theory (open symbols). The amplitude and x coordinate are in lattice units. The profiles were calculated after 480 MCS/site (top curve), 54 MCS/site (second curve), and 282 MCS/site (smallest amplitude curve), averaging over 2×10^5 realizations.

anisotropic surface free energy and mobility, one may improve the agreement. Actually, for the one-dimensional SOS model, the anisotropic surface free energy is known exactly,[25] and an upper bound has been determined for the adatom mobility,[10] which seems to be quite close to the true behavior.

Below roughening, the situation is less clear. For surface diffusion conflicting continuum theories have been proposed.[4,10,11] We did not attempt to clarify the controversy by this Monte Carlo study because of the large amount of computer time needed to obtain meaningful data, as mentioned above. Attention may be drawn to prior work on gratings, proposing simplified diffusion processes,[5] as well as recent impressive large-scale simulations, which, however, may have been performed too close to the roughening transition for too small sizes to draw firm conclusions about the generic scaling properties below roughening.[24] Instead, we considered evaporation dynamics.

As had been noted before,[5,9] the continuum description, Eq. (15), gives a rather unsatisfactory description of the simulated profile of 1D gratings with moderately large wavelengths, of up to about 100 to 200 lattice spacings, and quite small amplitudes, of about five or less lattice spacings. This discrepancy can be traced back to the dynamics at the top of the profile as discussed in the preceding section. Indeed, in continuum theory the vanishing mobility, following from nucleation processes,[2] on the top terraces gives rise to a nonparabolic sharpening near the top of the profile. However, the top-step annihilation process removes that peculiarity. Accordingly, even for gratings of wavelengths of up to 600 atomic spacings, new simulations do not show profile shapes sharper than parabolic at their apexes.[26]

For wire geometries of small size, the simulated profiles also differ significantly from those predicted by the continuum theory, as illustrated in Fig. 7. In particular, they do not exhibit the predicted nonparabolic sharpening, of exactly the same type as for gratings, but they are more rounded near the top, reflecting again the dynamics of top-step annihilation. At the sides they are leaner than those obtained by integrating the continuum theory, Eq. (15). The deviations from continuum theory become even larger as time goes on, i.e., at smaller amplitudes. A widening of the profiles, by increasing w_0 from 3 to 9, has only a minor effect on the shape differences (see Fig. 7).

In Fig. 5, the time dependence of the amplitude $A(t)$ for wires with the same initial profile, $A_0=w_0=3$, above and below roughening is shown, and compared to the predictions of the continuum theories, Eqs. (3) and (15). Below roughening, one finds drastic deviations, as shown by the behavior of the effective exponent $\tau(A)$. The continuum theory, Eq. (18), predicts a decay of the profile amplitude with τ approaching, at small amplitude, the asymptotic value $-\frac{1}{6}$. In the simulations, the healing proceeds much more rapidly. At monoatomic height, the relaxation slows down a little bit, but finally it seems to follow an exponential law (the exponential form may be reproduced in an easy way by considering an initial wire profile of height and width 1, at zero temperature).

Perhaps much wider profiles may be needed to approach a regime where the continuum theory provides a closer description of the simulational data for the temporal decay of the amplitude. We therefore increased the width of the initial profile, up to values for which reliable data could be obtained in reasonable computing times.

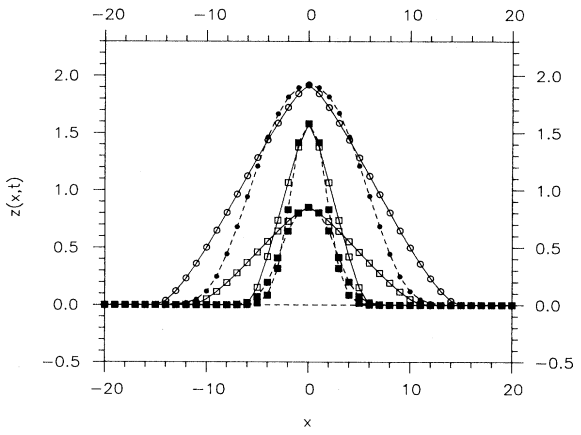

FIG. 7. Wire profiles of the two-dimensional SOS model, with $A_0=w_0=3$ (squares), and with $A_0=3$ and $w_0=9$ (circles) below roughening, $k_BT/J=0.8$, comparing simulational data (full symbols, broken lines) to the corresponding numerical solutions of the continuum theory, Eq. (15) (open circles, solid lines), for evaporation kinetics. The amplitude and x coordinates are in lattice units. The profiles were calculated after 205 MCS/site (top curve), 29 MCS/site (second curve), and 62 MCS/site (lowest amplitude curve), averaging over 2×10^4 realizations.

The amplitude was kept fixed, $A_0=3$, and we varied w_0 from 3 to 9, with $(2K+1)$ increasing from 41 to 81, $L=41$. In Fig. 8, the effective exponent τ is depicted. The relaxation gets slower as the width increases, but deviations from continuum theory are still significant. Plotting $\tau(w)$, at fixed height, a rather nontrivial behavior is revealed; an extrapolation to large values of w seems to be quite speculative, not allowing us to rule out or confirm the asymptotic decay law predicted by continuum theory. Obviously, rather large correction terms, in the mobility and the surface free energy, may be needed to describe the Monte Carlo data. Indeed, the terms of these two quantities seem to be of decisively different origin and relevance. As mentioned above and before, the mobility is always dominated by step dynamics, thereby avoiding its vanishing at flat surfaces, while only usual finite-size corrections affect the singularity in the surface free energy. In addition, drastic differences in the amount of mass change during the relaxation process, comparing the continuum theory and simulations, also play an important role (see below).

Moreover, pronounced lattice effects are observed in the simulated decay process, which have not been taken into account by the continuum theory. They become, at small amplitudes, more noticeable as the profile gets wider: At profiles of integer height, here 1 and 2, the relaxation process slows down (see Fig. 8), reflecting the smoothness of the top layer below roughening, with the equilibration proceeding layer by layer. As for gratings (periodic grooves),[5] there are a slow time scale, due to the meandering of the steps bounding the top terrace, and a fast time scale, associated with the islanding, as illustrated by the top-step annihilation process described in the preceding section.

We obtained similar results for larger amplitudes, up to $A_0=10$, with the effective exponent τ increasing somewhat, but being still rather far from the behavior predicted by the continuum theory. The profiles remained rounded near the top.

As indicated before, the large differences between the simulated and predicted profiles can be partly explained by the fact that the continuum theory, Eq. (15), implies a conservation of excess mass, being initially A_0w_0, while in the simulations, the flat surface with vanishing excess mass is approached (in contrast, we observe even a slight increase in the excess mass for the one-dimensional case); see Fig. 9. Therefore, we did some simulations with mass conservation, removing and adding particles simultaneously at randomly chosen sites,[5] for wires below roughening. However, as before, the simulated profiles remained rounded at the top, in marked contrast to the nonparabolic sharpening predicted by continuum theory. The temporal decay, for small wires, also did not agree with the predicted one, and a rather cumbersome finite-size scaling analysis may be needed to establish the asymptotic decay law. Above roughening, simulational data for the one-dimensional SOS model with mass conservation show the expected close similarity to the profiles obtained from continuum theory using the same starting configuration, with even a slight improvement compared to the case of Glauber kinetics without mass conservation.

B. Square bumps

We now consider the relaxation of square bumps with the initial configuration,

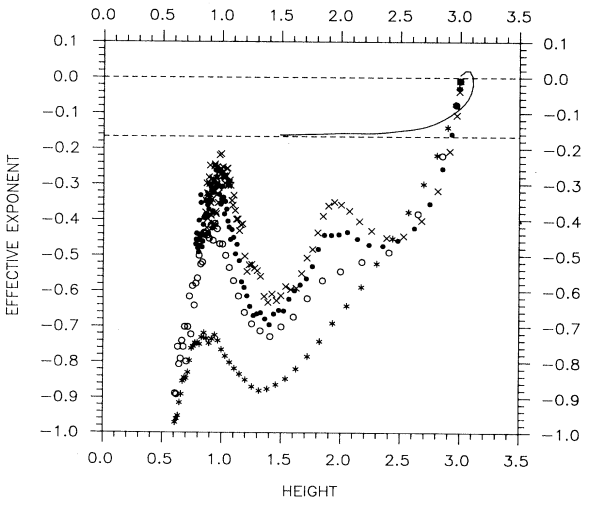

FIG. 8. The effective exponent Eq. (28) versus height of the wire profile simulated for the two-dimensional SOS model below roughening, at $k_BT/J=0.8$, for wires of different initial widths, $w_0=3$ (asterisks), 5 (open circles), 7 (full dots), and 9 (crosses), at fixed initial amplitude, $A_0=3$. For comparison, the result of the continuum theory, $w_0=A_0=3$, is shown (solid line). Evaporation kinetics is considered.

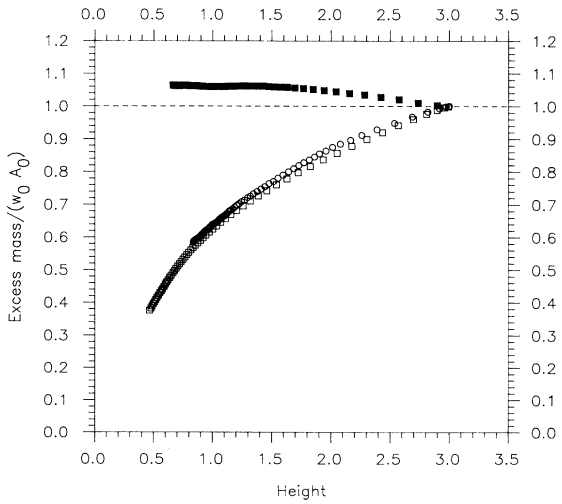

FIG. 9. Simulated excess mass for wires above (full squares) and below (open symbols) roughening, for the one-dimensional case with $w_0=A_0=3$ and the two-dimensional case with $A_0=3$ and $w_0=3$ (circles), as well as $w_0=9$ (squares), always at $k_BT/J=0.8$, for evaporation kinetics.

$$h(x,y,t=0)=\begin{cases}A_0, & |x|\le M,\ |y|\le M\\ 0, & \text{elsewhere}\end{cases} \tag{29}$$

placed on square surfaces of $N=(2K+1)\times(2K+1)$ sites, using full periodic boundary conditions. In particular, the average profile through the center, say, $z(x,y=0,t)$, was recorded. Simulations were performed above, $k_BT/J=2.0$, and below, $k_BT/J=0.8$, the roughening transition temperature of the SOS model, Eq. (25). The width of the bump, $w_0=2M+1$, ranged from 3 to 41, with $(2K+1)$ varying from 41 to 101. The amplitude A_0 was usually chosen to be 3 to 5. Typically, we sampled over 10^4 to 10^5 realizations. Simulations were done using Glauber kinetics to mimic evaporation dynamics, above and below roughening; surface diffusion was simulated only above roughening.

Above roughening, in the case of evaporation kinetics, the capillary theory of Mullins[1,17] described well the simulated profile shapes (see Fig. 10), even for small bumps, with, say, $w_0=A_0=3$. As in the case of 1D wires, the agreement improve further at lower amplitude and for wider bumps. The predicted asymptotic decay of the amplitude, as t^{-1} [see Eq. (8)], is also reached closely in the simulations, e.g., at $A_0=w_0=3$, when the amplitude $A(t)$ gets smaller than, roughly, 1. The decay is much quicker than for 1D wires, leading to a less rapid spreading of the profile, at fixed height (compare Figs. 4 and 10). As noticed above and before, the continuum theory may be improved by introducing anisotropic surface free energy and mobility to describe the Monte Carlo data, but the agreement is already satisfying.

Similarly, for surface diffusion above roughening, the classical continuum theory describes closely the simulated profiles, predicting correctly its oscillatory behavior (which is even more subtle than for the wire geometry). An example is depicted in Fig. 11, for a small bump with $A_0=w_0=3$, showing the very close similarity.

Below roughening, the bumps, at low amplitude, are expected to decay and shrink simultaneously, following continuum theory and step models.[2] Indeed, the simulations confirm this prediction qualitatively (see Fig. 12). Good quantitative agreement can be demonstrated by analyzing the scaling behavior of the profile obtained from the continuum theory, Eq. (20), for radially symmetric bumps at late stages of the healing process. For instance, the profiles of the case depicted in Fig. 12, $w_0=21$ and $A_0=3$, nicely follow that scaling form of Eq. (20) at small amplitudes (this has been tested by recording the times and radial distances of the profile at constant height; e.g., at 0.5, the scaling behavior is clearly fulfilled at amplitudes smaller than about 1.2). At large amplitudes, the observed deviations from the scaling form reflect step-step interactions, which are not taken into account in Eq. (20), and which are the reason for the spreading of the foot of the profile at early times.

In addition, strong lattice effects which have not been captured by the continuum theory show up also for the bumps. For instance, by increasing the initial width w_0, the effective exponent τ versus height displays a more and more pronounced nonmonotonic behavior, similar to that depicted in Fig. 8. Again, the relaxation process tends to get slowed down when the height of the profile is close to an integer value, due to the smoothness of the top layer. A similar behavior has been observed recently experimentally on Pb(111) and Au(111) surfaces, monitoring the flattening of a bump using STM.[27]

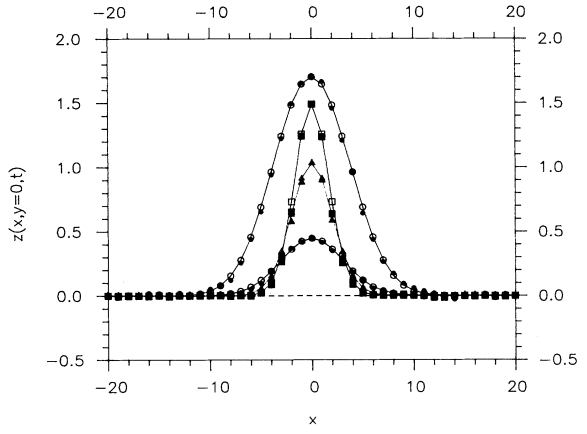

FIG. 10. Simulated bump profiles (full symbols) of the two-dimensional SOS model above roughening, $k_BT/J=2.0$, with $w_0=A_0=3$ as well as $A_0=3$ and $w_0=7$ (upper case), compared to continuum theory (open circles, solid lines), for evaporation kinetics. The amplitude and x coordinate are in lattice units. The profiles were calculated after 58 MCS/site (top curve), 15 MCS/site (second curve), 23 MCS/site (third curve), and 54 MCS/site (lowest amplitude curve), averaging over 10^4 realizations.

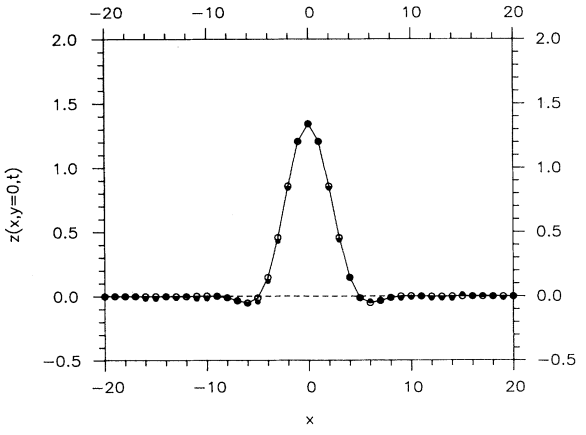

FIG. 11. Simulated bump profile (full symbols) of the two-dimensional SOS model above roughening, $k_BT/J=2.0$, with $w_0=3$ and $A_0=3$, for surface diffusion, compared to continuum theory (open circles, solid line). The amplitude and x coordinate are in lattice units. The curve was calculated after 62 MCS/site, averaging over 10^4 realizations.

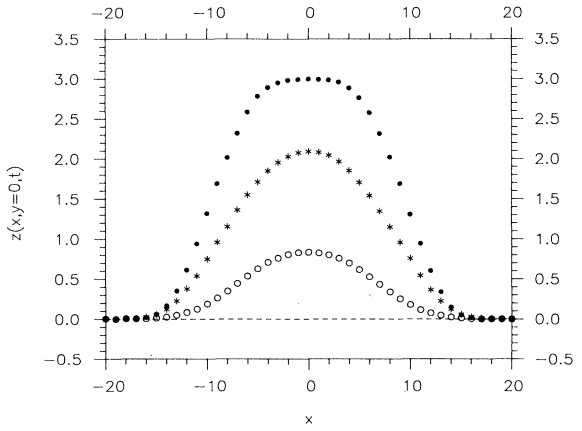

FIG. 12. Simulated bump profiles of the two-dimensional SOS model below roughening, $k_BT/J=0.8$, with $w_0=21$ and $A_0=3$, for evaporation kinetics. The amplitude and x coordinate are in lattice units. The curves were calculated after 12 MCS/site (top curve), 246 MCS/site (second curve), and 480 MCS/site (bottom curve), averaging over 4×10^3 realizations.

V. SUMMARY

We have compared continuum theories, step models, and Monte Carlo simulations for the decay of several types of nonequilibrium surface profiles. Above roughening, the Monte Carlo simulations confirm the predictions of Mullins' asymptotic continuum theory, both for surface diffusion (see Figs. 6 and 11) and evaporation kinetics (see Figs. 4 and 10). Small deviations are well understood and may be mainly attributed to anisotropies in the mobility and the surface free energy. The Monte Carlo simulations show the predicted profile shapes, including the oscillatory profile shapes characteristic of surface diffusion (see Figs. 6 and 11), and they reproduce the asymptotic temporal decay laws of the amplitude (see Figs. 5 and 8).

Below roughening, we concentrated on evaporation recondensation, and showed that the rounding of the mobility and surface free energy leads to the possibility of finding sharpening, broadening, and sinusoidal profiles (see Fig. 2). We also discussed the process of top-step annihilation, which removes the sharp profiles predicted by the continuum theory (15) for the 1D wire and 1D grating profiles decay (see Fig. 7). A simulation using Langevin dynamics shows the characteristic features of island nucleation and shrinking (see Fig. 3). The typical time taken for the top terrace (of width W) to disappear is proportional to W^4, and it is seen that the two top steps interact with each other over significant distances.

The results of the Monte Carlo simulations below roughening deviate from some of the predictions of the continuum theory assuming a vanishing mobility at the top of the profiles. For example, for the wire case, the profiles do not show the peculiar nonparabolic sharpening at their tops (see Fig. 7). This does not mean that the continuum theory is basically incorrect (on the contrary, the basic structure has been convincingly established by Spohn), but is indicates that a more adequate form of the mobility has to be incorporated. The effective decay exponent displays quite large oscillations (see Figs. 5 and 8), reflecting strong lattice effects, which are not described by the continuum theory. We also note that the mass is not conserved in the simulations (Fig. 9), but it is in the continuum theory.

On the other hand, for the bump case (Fig. 12) the observed scaling behavior of the profile at small amplitudes is consistent with the continuum theory. In that case, the top terrace dynamics is not important.

In conclusion, it is seen that Monte Carlo simulations above roughening recover the predictions of continuum theory for perturbations even of small extent. In contrast, below roughening there are a variety of factors which make comparison of continuum theory with lattice models problematic. We attempted to identify them and described partial resolutions of them in this article.

ACKNOWLEDGMENTS

It is a pleasure to thank H. P. Bonzel, J. Krug, and W. W. Mullins for very useful discussions. H. T. Dobbs helped us, kindly and efficiently, with the integration of some of the classical continuum equations. We thank L.-H. Tang for informing us about his simulational data for grooves prior to publication. Stimulating conversations at the W. E. Heraeus seminar in Bad Honnef, Germany, May 1995, with many of the experts on the subject of this article are gratefully acknowledged. P.M.D. thanks the Humboldt Foundation and the NSF under Contract No. DMR-931 2839 for support. He is also grateful for the support and hospitality of the Forschungszentrum Jülich during a visit when this work was initiated.

[1]W. W. Mullins, J. Appl. Phys. **30**, 77 (1959).
[2]H. Spohn, J. Phys. I (France) **3**, 69 (1993); J. Hager and H. Spohn, Surf. Sci. **324**, 365 (1995).
[3]H. P. Bonzel, U. Breuer, B. Voigtländer, and E. Zeldov, Surf. Sci. **272**, 10 (1992).
[4]C. C. Umbach, M. E. Keeffe, and J. M. Blakely, J. Vac. Sci. Technol. A **9**, 1014 (1991); M. E. Keeffe, C. C. Umbach, and J. M. Blakely, J. Phys. Chem. Solids **55**, 965 (1994).
[5]W. Selke and T. Bieker, Surf. Sci. **281**, 163 (1993).
[6]W. Selke and P. M. Duxbury, Acta Phys. Slovaca **44**, 215 (1994).
[7]W. Selke and J. Oitmaa, Surf. Sci. **198**, L346 (1988).
[8]Z. Jiang and C. Ebner, Phys. Rev. B **40**, 316 (1989).
[9]W. Selke and P. M. Duxbury, Z. Phys. B **94**, 311 (1994).
[10]J. Krug, H. T. Dobbs, and S. Majaniemi, Z. Phys. B **97**, 281 (1995).
[11]F. Lançon and J. Villain, in *Kinetics of Ordering and Growth at Surfaces*, edited by M. G. Lagally (Plenum, New York,

1990).
[12]A. Rettori and J. Villain, J. Phys. (Paris) **49**, 257 (1988).
[13]M. Ozdemir and A. Zangwill, Phys. Rev. B **42**, 5013 (1990).
[14]M. A. Dubson, M. Kalke, and J. Hwang, Phys. Rev. B **47**, 10044 (1993); M. A. Dubson and G. Jeffers, *ibid.* **49**, 8347 (1994).
[15]H. P. Bonzel, E. Preuss, and B. Steffen, Appl. Phys. A **35**, 1 (1984); H. P. Bonzel and E. Preuss, Surf. Sci. **336**, 209 (1995).
[16]J. W. Cahn and J. E. Taylor, Acta Metall. Mater. **42**, 1045 (1994).
[17]W. W. Mullins, in *Metal Surfaces: Structure, Energetics and Kinetics,* edited by R. Vanselow and R. Howe (Springer, New York, 1963), p. 17.
[18]P. J. Upton and D. B. Abraham, Phys. Rev. B **39**, 9650 (1989); R. Lipowsky, J. Phys. A **18**, L585 (1985); S. F. Edwards and D. R. Wilkinson, Proc. R. Soc. London Ser. A **381**, 17 (1982).
[19]N. C. Bartelt, J. L. Goldberg, T. L. Einstein, and E. D. Williams, Surf. Sci. **273**, 252 (1992).
[20]L. Kuipers, M. S. Hogemann, and J. W. M. Frenken, Phys. Rev. Lett. **71**, 3517 (1993).
[21]M. Giesen-Seibert, R. Jentjens, M. Poensgen, and H. Ibach, Phys. Rev. Lett. **71**, 3521 (1993).
[22]A. Pimpinelli, J. Villain, D. E. Wolf, J. J. Metois, J. C. Heyraud, I. Elkinani, and G. Uimin, Surf. Sci. **295**, 143 (1993); N. C. Bartelt, T. L. Einstein, and E. D. Williams, *ibid.* **312**, 411 (1994).
[23]J. D. Weeks, in *Ordering of Strongly Fluctuating Condensed Matter Systems,* edited by T. Riste (Plenum, New York, 1980).
[24]P. C. Searson, R. Li, and K. Sieradzki, Phys. Rev. Lett. **74**, 1395 (1995).
[25]C. Rottman and M. Wortis, Phys. Rev. B **24**, 6274 (1981).
[26]L.-H. Tang (private communication).
[27]D. R. Peale and B. H. Cooper, J. Vac. Sci. Technol. A **10**, 2210 (1992); L. Kuipers, Ph.D. thesis, University of Amsterdam, 1994.